[Frontiers in Bioscience 10, 1693-1706, May 1, 2005]

EVIDENCE FOR SIMULTANEOUS $1Na^+$:$1Mg^{2+}$ AND PING PONG $2Na^+$:$1Mg^{2+}$ EXCHANGERS IN RAT THYMOCYTES

Constanza Contreras-Jurado [1], Nuria Sanchez-Morito [1], Anabel Ruiz-Contreras [1], Marco T. Gonzalez-Martinez [2] and Agatangelo Soler-Diaz [1,3]

[1] Departamento de Fisiologia, Facultad de Medicina, Avenida Madrid 13 E 18012, Universidad de Granada, (Spain, [2] Departamento de Farmacologia, Facultad de Medicina, Universidad Nacional Autonoma de Mexico, Mexico, [3] Instituto de Biotecnologia, Campus de Fuentenueva, Universidad de Granada, Spain

TABLE OF CONTENTS

1. Abstract
2. Introduction
3. Materials and methods
- *3.1. Materials and media*
  - *3.1.1. Preparation of thymocytes*
- *3.2. Mg^{2+} loading procedure*
- *3.3. Measurement of intracellular Na^+ and Mg^{2+}*
- *3.4. Measurement of Na^+_o-induced Mg^{2+} efflux*
- *3.5. Measurement of Na^+_o-induced Mg^{2+}_{it} and Na^+_{it} changes*
- *3.6. Statistical analysis*

4. Results
- *4.1. Na^+_{it} and Mg^{2+}_{it} content*
- *4.2. Plasmalemmal Mg^{2+} leak was not enhanced by A-23187 Mg^{2+} loading*
- *4.3. Na^+_o-induced Mg^{2+} efflux in fresh and Mg^{2+}-loaded thymocytes*
- *4.4. Dependence of Na^+_o-induced Mg^{2+} efflux on internal Mg^{2+}_{it}*
- *4.5. Induction of Mg^{2+}_{it} decrease and Na^{2+}_{it} increase by Na^+_o in Mg^{2+}-loaded thymocytes*
- *4.6. Inhibition by amiloride of either Na^+_o-induced Mg^{2+} efflux and Na^+_o-induced Na^+ influx in Mg^{2+}-loaded thymocytes*
- *4.7. Dependence of the $V_{Mg}(Na)_{max}/K_{Na}$ ratio to the internal Mg^{2+} content*
- *4.8. Thermodynamics of the Na^+/Mg^{2+} exchange*

5. Discussion
- *5.1. Simultaneous versus ping-pong exchange*
- *5.2. Physiological roles of ping pong and simultaneous Na^+/Mg^{2+} exchangers coexisting in the same cel*
- *5.3. Appendix: the kinetics of a bisubstrate exchanger*

6. Acknowledgments
7. References

1. ABSTRACT

Rat thymocytes showed two Na^+/Mg^{2+} exchangers with high- and low- affinities for external Na^+ (Na^+_o) at physiological internal Mg^{2+}content. The total internal Mg^{2+} content (Mg^{2+}_{it}) was enhanced by loading with $MgCl_2$ and the ionophore A-23187. Under these conditions, Na^+/Mg^{2+} exchangers were dramatically stimulated by the Mg^{2+}_{it} increase. Na^+-induced Mg^{2+} effluxes were independent of Cl^-_o or H^+. The Na^+/Mg^{2+} exchangers, which we named HANao (high affinity for Na^+_o) and LANao (low affinity for Na^+_o), were dissected in Mg^{2+}-loaded thymocytes according to their kinetics and stoichiometries. HANao, which showed an apparent dissociation constant for Na^+_o ($K_{Na\ H}$) = 9.2 +/- 1.6 mmol l^{-1} Na^+_o and a maximal Na^+ influx rate ($V_{Na}(Na_H)_{max}$) = 30.5 +/- 6.1 mmol (l cells)$^{-1}$ h^{-1}, was a $1Na^+$:$1Mg^{2+}$ simultaneous antiporter insensitive to external magnesium (Mg^{2+}_o) whereas that LANao, with $K_{Na\ L}$ = 65.1 +/- 8.6 mmol l^{-1} Na^+ and a $V_{Na}(Na_L)_{max}$ = 79.5 +/- 14.3 mmol (l cells)$^{-1}$ Na^+ h^{-1}, was a $2Na^+$:$1Mg^{2+}$ "ping-pong" antiporter which was strongly inhibited by Mg^{2+}_o. At physiological concentration of Mg^{2+}_o (1 mM), the Na^+/Mg^{2+} exchange through the LANao was inhibited by ~50%. Amiloride (10^{-4} M) inhibited at similar extent both Na^+ and Mg^{2+} fluxes at high and at low Na^+_o.

2. INTRODUCTION

Intracellular magnesium plays a central role in animal cells since it modulates a myriad of biochemical processes. For instance, Mg^{2+} is required for the function of numerous enzymes (phosphatases, ATPases and RNA polymerases), it is essential for the structural integrity of ribosomes (1), it may affect mitochondrial enzymes and transporters and its accumulation in mitochondria depends on the respiratory phase (2). Mg^{2+} influences apoptosis (3), may modulate transcription process (4), and regulates the activity of potassium channels (5) and ryanodine receptors (6).

It is well known that free cytosolic Mg^{2+} is maintained far from its electrochemical equilibrium. Indeed, according to the Nernst equation, for an excitable cell like the cardiomyocyte with *E*m = -70 mV and a free external Mg^{2+} of 1 mM the expected free cytosolic Mg^{2+} at equilibrium should be ~188 mM. However, free cytosolic Mg^{2+} is 0.5 to 1 mM, while the total internal magnesium

content is ~10 mM. In addition, free Mg^{2+} is ~1 mM in the mitochondria and the sarcoplasmic reticulum (7). This evidence indicates that magnesium extruding mechanisms present in the plasma membrane must be permanently active in order to maintain a low free intracellular concentration.

The transport systems that regulate the internal Mg^{2+} concentration are poorly understood and none of them have been cloned or isolated. It has been proposed that Na^+/Mg^{2+} exchangers are the major extruding magnesium systems (7-9). Variants of the Na^+_o-induced Mg^{2+} transport systems differ in the stoichiometry of the exchange, in the capability of a reverse mode of operation and in the sensitivity to inhibitors. As for the stoichiometry, several kinds of exchangers have been reported, either the electrogenic $1Na^+/1Mg^{2+}$ (9) and $3Na^+/1Mg^{2+}$ (10, 11) or the electroneutral $2Na^+/1Mg^{2+}$ in human (12) and rat (13) red blood cells and rat thymocytes (14). A $2Na^+$, $2K^+$, $2Cl^-/1Mg^{2+}$ antiporter was reported in barnacle muscle and squid axons (15). Furthermore, two different Na^+/Mg^{2+} exchangers are exclusively present at apical and basolateral poles in rat hepatocytes (16, 17).

If the Na^+/Mg^{2+} exchange is electrogenic, changes in membrane potential should affect the rate of Mg^{2+} exchange. In this regard, we recently provided evidence, based on the effect of membrane potential on the rate of exchange activity (18), that rat thymocytes may be endowed with Na^+/Mg^{2+} exchangers with $1Na^+:1Mg^{2+}$; $2Na^+:1Mg^{2+}$ and $3Na^+:1Mg^{2+}$ stoichiometries. Interestingly, their activity, which strongly depends on the free cytosolic Mg^{2+}, is differentially affected by the external sodium concentration. These experiments were done by measuring the Na^+_o-induced Magfura-2 fluorescence decay in calcium-depleted thymocytes and the activity could only be observed when the total internal Mg^{2+} content (and subsequently cytosolic Mg^{2+}) was enhanced above the physiological level (18).

In this work, we studied the Na^+/Mg^{2+} exchange through the analysis of Mg^{2+} on the external medium and the analysis of the increase on the Na^+ internal content, We have dissected two exchangers through the kinetical analysis of Na^+_o –induced Mg^{2+} efflux saturation curves in thymocytes with normal and enhanced Mg^{2+} content. We have quantitatively determined the stoichiometries of the Na^+/Mg^{2+} exchangers present in rat thymocytes through the analysis of Na^+ and Mg^{2+} coupled fluxes. We confirm that these cells have Na^+/Mg^{2+} exchangers with different stoichiometries and unveil mechanistic properties through the kinetics analysis of Na^+ and Mg^{2+} coupled fluxes.

3. MATERIALS AND METHODS

3.1. Materials and media

Male Wistar rats weighing 150-200 g were housed under adequate and constant temperature, humidity and photoperiod. Rats were fed a standard diet and were given tap water. Chemicals were of the purest analytical grade (Sigma or Aldrich, Steinheim Germany; Merck, Darmstadt Germany). A-23187, BSA and MOPS were from Sigma. The media (Na^+ -medium) used had the following composition (in mM): 150 NaCl, 5 KCl, 10 glucose, 10 MOPS-Tris, (pH 7.4 at 37ºC). The choline medium had the same composition except that NaCl was replaced with choline Cl^-. The osmolality of all media was adjusted to 300 ± 5 mosm kg^{-1} by adding concentrate solutions of the main components. The osmometer was calibrated with 0, 300, and 1000 mosm kg^{-1} reference standards. (Osmostat M-6020, Daichi Kagaku Co. Ltd. Kyoto Japan). All media were nominally free from Ba^{2+}, Sr^{2+}, Mg^{2+}or Mn^{2+} as determined by Atomic Absorption Spectrophotometry (AAS).

3.1.1. Preparation of thymocytes

Rat thymocytes were isolated as described (19), with some modifications. Briefly, rats were anesthetized by intraperitoneal injection of 50 mg kg^{-1} sodium pentobarbital. After disappearance of corneal and nociceptive reflexes, anaesthetized rats were laparatomized and exsanguinated by a cut on abdominal cava and aorta and the thymus was exposed by thoracotomy. Thymus glands from 6 to 12 rats were carefully and rapidly excised avoiding contamination with blood. Rats died under anesthesia during or immediately after thymus excision. Glands were washed twice at 20ºC in Na^+ -medium (pH 7.4 at 20ºC) and homogenized in 30 ml of the same medium using seven passes with a loose-fitting glass pestle (Pobel, Madrid, Spain). Each cell suspension was filtered through a thin mesh and impurities were left to sediment for five minutes. Supernatants with cells were recovered and centrifuged at 800 g and 20ºC for 5 minutes (RF Varifuge, Heraeus Sepatech, Germany). The pellet was resuspended in choline medium (pH 7.4 at 20ºC) and washed twice by centrifugation under the same conditions. Small aggregates were removed and cells were weighted and finally resuspended at 10% w/v and mixed in choline medium. The resultant pool was stored at 20ºC. Four small aliquots of each cell suspension were taken for thymocryte capillary measurement (Heraeus Sepatech, Germany) and for Mg^{2+}_{it} and Na^+_{it} measurement by AAS and AES, respectively Perkin Elmer 3100 Spectrophotometer, Shelton CT, USA).

3.2. Mg^{2+} loading procedure

Washed cells were resuspended at 10% w/v in choline medium supplemented with 12 mM Mg^{2+} + 40 µM A-23187. The suspension was gently shaken by repeated pipetting and incubated for 20 min at 20ºC. Cells were centrifuged (5 min at 1200 g and 20ºC), resuspended and washed two times at 37ºC in choline medium + 12 mM Mg^{2+} + 1% w/v BSA to remove the ionophore and then washed twice in choline medium + 1% w/v BSA to remove external Mg^{2+}. Finally, cells were centrifuged and washed three times in cold choline medium (pH 7.4 at 4ºC) to remove both BSA and residual external Mg^{2+}. The resultant Mg^{2+}-loaded cells were stored at 4ºC. Aliquots were taken for thymocryte and for Na^+_{it} and Mg^{2+}_{it} determinations by triplicate. In five experiments the loading procedure was modified to obtain two subsets of a same pool of cells with high and low Mg^{2+}_{it}. The low Mg^{2+}_{it} subset was loaded in choline medium with 6 mM Mg^{2+} + 20 µM A-23187. In some experiments the loading procedure was done in the presence of 10 µM of the Na^+,K^+/H^+ ionophore nigericin.

This ionophore shortened the loading time without affecting the final Mg^{2+}_{it} or the transport rates (not shown). This ionophore was removed, along with A23187, from the cells by BSA incubation. Cell viability was higher than 95% in Mg^{2+}-loaded thymocytes, as assessed by Trypan blue (Merck-Darmstadt Germany) exclusion test.

The thymocryte of the cell suspension was measured by using capillaries (Vitrex Herlev, Denmark), that were centrifuged for 10 min at 13,000 g (Haemofuge A, Heraeus Sepatech) and the cells and supernatants columns were measured by a digital calliper. The thymocryte of the suspension was corrected by the trapped extracellular media factor (0.40%) and water content (76.4 ± 0.8%) according to (20). In addition to thymocryte measurement, cell counting with a Neubauer hematocytometer (Sigma, Madrid Spain) was performed as control of viability (Trypan blue, Merck-Darmstadt Germany) for each block of experiments. We previously reported that the average cell volume of rat thymocytes is 128.3 ± 5.1 μm^3 (21). Relative volume changes, estimated as the ratio between the thymocryte and the number of cells, did not exceed 5%.

3.3. Measurement of intracellular Na^+ and Mg^{2+}

Intracellular magnesium (Mg^{2+}_{it}) and intracellular sodium (Na^+_{it}) in fresh or Mg^{2+}-loaded thymocytes were determined in three aliquots of washed cell suspensions that were lysed in a Mg^{2+}-free digitonin (0.01%) + 5 % w/v trichloroacetic acid solution. The Na^+ content (in mmol (l cells)$^{-1}$) was calculated by dividing the Na^+ Atomic Emission Spectrophotometry (AES) reading (see below) by the thymocryte. The total cell Mg^{2+} content (in mmol (l cells)$^{-1}$) was calculated by dividing the Mg^{2+} Atomic Absorption Spectrophotometry (AAS) reading (see below) by the thymocryte (12).

3.4. Measurement of Na^+_o-induced Mg^{2+} efflux

The efflux of Mg^{2+} induced by external Na^+ was assessed as the difference between $[Mg]^{2+}$ detected in the medium (supernatants) from cells incubated in Na^+ -containing medium minus the $[Mg^{2+}]$ detected in the medium (supernatants) from the same pool of cells incubated in choline medium. Aliquots of 100 µl of the cell suspension (fresh or Mg^{2+}-loaded thymocytes) were added to series of cold (4ºC) duplicate tubes containing either 1 ml Na^+ -medium, 1 ml choline-medium or 1 ml of a mixture of them (see figure legends). To start the exchange reaction the tubes were introduced in the incubation bath at 37ºC, for different time periods. The incubation period varied depending on the experiment (see figure legends) and was chosen to obtain reliable initial rate conditions. After incubation, cell suspensions were cooled (4ºC) for 1 min and immediately centrifuged at 4ºC and 800 g for 5 min. The specific Na^+_o–induced Mg^{2+} efflux was obtained from the difference between Na^+ and choline or N-methyl D-glucamine media.

3.5. Measurement of Na^+_o-induced Mg^{2+}_{it} and Na^+_{it} changes

Aliquots of Mg^{2+}-loaded cell suspension (200 µl) were added cold tubes (triplicates) containing 2 ml of a mixture of Na^+ -medium and choline-medium (pH 7.4 at 37º C). The Na^+_o in the incubation media were 0, 3, 5, 10, 15, 20, 30, 45, 55, 65, 75, 90, 120 and 150 mmol l^{-1}. The tubes (triplicates for each Na^+_o concentration) were gently shaken before starting the exchange reaction at 37ºC. After incubation, cell suspensions were cooled (4ºC) for 1 min and immediately centrifuged at 4ºC and 800 g for 5 min. Supernatants were discarded and pellets were washed three times with cold choline-medium (pH 7.4 at 4ºC). Cells were lysed in 0.01% w/v digitonin and 5% w/v TCA was added before centrifugation at 3000 g. Supernatants were transferred for Mg^{2+}_{it} and Na^+_{it} measurements by AAS and AES, respectively (see below). Mg^{2+}_{it} (in mmol (l cells)$^{-1}$) was calculated by dividing the AAE reading by the % of cells present in the incubated suspension (i.e. 1/6 of the thymocryte). Na^+_{it} (in mmol (l cells)$^{-1}$) was calculated by dividing the AES reading by the % of cells present in the same incubated suspension.

Magnesium was measured by AAS in the presence of 0.1% $LaCl_3$ at 285.2 nm (Perkin-Elmer 3100 spectrophotometer) and Na^+ was measured in the presence of 0.1% CsCl by AES at 589 nm (Perkin-Elmer 3100 spectrophotometer).

3.6. Statistical analysis

Data are presented as mean ± SE. $p<0.05$ was considered statistically significant. Data were analyzed by one-way ANOVA and multiple means were compared by the Student-Newman-Keuls method. Normal distribution was tested by Shapiro-Wilkinson, skewness and kurtosis contrast tests. Linear regression with comparison of intercepts and slopes, and non-linear regression by the iterative Levemberg-Marquardt algorithm, that was employed to fit Na^+-induced Mg^{2+} efflux and Na^+-induced Na^+ influx curves, were made by using the Statgraphics plus v.4.1 package (Statistical Graphics Com., Rockville MD).

4. RESULTS

4.1. Na^+_{it} and Mg^{2+}_{it} content

The basal (resting) Mg^{2+}_{it} and Na^+_{it} in normal (fresh) thymocytes were 10.4 ± 0.4 mmol (l cell)$^{-1}$ and 9.9 ± 0.8 mmol (l cell)$^{-1}$ (n=14), respectively. After Mg^{2+} -loading, Mg^{2+}_{it} raised to 19.6 ± 0.8 mmol (l cells)$^{-1}$ (n=26) without significant change in Na^+_{it} (8.5 ± 0.9 mmol (l cell)$^{-1}$, n=26). Both Mg^{2+}_{it} and Na^+_{it} fitted unimodal normal distribution ($p<0.05$, Shapiro-Wilkinson test) in both normal and loaded thymocytes, indicating that the sample was homogeneous.

4.2. Plasmalemmal Mg^{2+} leak was not enhanced by A-23187 Mg^{2+} loading

The use of A-23187 to load rat thymocytes with high internal Mg^{2+} was first reported by Günther and Vormann (22). Even if this ionophore does not catalyze fluxes of single monovalent cations (23), it could be argued that Mg^{2+} leak through residual A-23187 could impair the Mg^{2+} signal-noise ratio. Transport through A-23187 is electroneutral and it exchanges Mg^{2+}_o for $2H^+_i$, so that the equilibrium is reached when (24):

$$[H^+]_i^2 / [H^+]_o^2 = [Mg^{2+}]_i / [Mg^{2+}]_o.$$

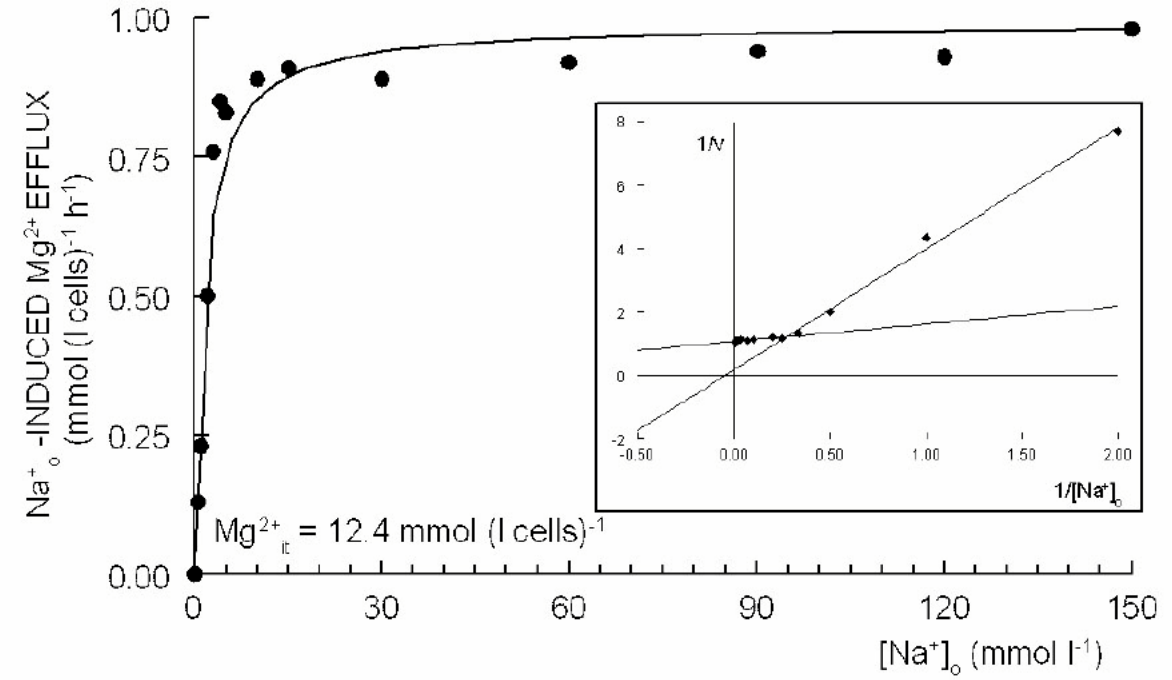

Figure 1. Effect of isotonic Na^+_o on Na^+_o–induced Mg^{2+} efflux in fresh thymocytes (not Mg^{2+}-loaded). Samples of cells maintained in choline medium were centrifuged and resuspended in choline-NaCl isotonic mixtures at 37°C. After 10 minutes, the cells were centrifuged and the Mg^{2+} content present in supernatants determined. The incubation time was chosen since in time-course experiments the initial activity was kept linear for 20 minutes (not shown). Each point is the mean of two single cell tubes. Inset: Double reciprocal (Lineweaver-Burk) plot of these data shows two regression lines with different slopes for high and low $[Na^+]_o$. At low Na^+_o, the reciprocal of Mg^{2+} efflux fitted the equation $1/V_{Mg}(Na) = 0.17 + 3.82\ 1/[Na^+]_o$, ($r = 0.9934$, $p<0.01$), while at high Na^+_o, the reciprocal of Mg^{2+} efflux fitted $1/V_{Mg}(Na) = 1.06 + 0.55\ 1/[Na^+]_o$, ($r = 0.7757$, $p<0.01$) This graph is representative of 4 experiments.

After loading, A-23187 can be effectively removed from the membrane by washing with BSA-containing media (24, 25). To confirm this, we tested whether residual A-23187 in the membrane could catalyze outward Mg^{2+} leak from Mg^{2+}-loaded thymocytes in choline medium. There was no Na^+_o -independent Mg^{2+} efflux increase for 5 min, even when the external H^+ concentration was raised 6.3 times (from pH = 7.4 to pH = 6.6). Moreover, the addition of A-23187 to the medium to a final concentration of 3.8×10^{-7} M (mimicking the effect of enhanced residual ionophore remaining on cells) did not further enhance Na^+_o –independent Mg^{2+} output at either pH 7.4 or pH 6.6 (not shown). These results agreed with our previous findings in Magfura2 –loaded rat thymocytes. We did not find a significant increase in cell autofluorescence, even when the highly fluorescent A-23187 was also used to load the cells (18).

4.3. Na^+_o-induced Mg^{2+} efflux in fresh and Mg^{2+}-loaded thymocytes

The efflux induced by 150 mmol l^{-1} Na^+_o in fresh cells was linear for 20 min and the initial rate was 1.9 ± 0.3 mmol Mg^{2+} (l cells)$^{-1}$ h^{-1}, (n=3). In Mg^{2+}-loaded cells, the Na^+-induced Mg^{2+} efflux was remarkably faster and larger. In these cells (Mg^{2+}-loaded thymocytes) the Mg^{2+} efflux induced by 150 mM Na^+_o increased linearly for 5 minutes and the initial rate was 10.24 ± 1.06 mmol Mg^{2+} (l cells)$^{-1}$ h^{-1} (n=4). Magnesium efflux in choline medium was negligible in fresh cells. In Mg^{2+}-loaded cells incubated for 5 min, the Mg^{2+} efflux measured in choline medium was ~3.6% of the flux measured in 150 mM Na^+_o medium. The Mg^{2+} efflux induced by Na^+ in Mg^{2+}-loaded thymocytes was not significantly affected by replacing external chloride by NO_3^- or by replacing choline by N-methyl D-glucamine (not shown). Furthermore, the external pH (6.8, 7.4, and 8.0) did not significantly affect it (not shown). Altogether, these evidence indicated that only Na^+ and Mg^{2+} were exchanged.

In fresh thymocytes, the curve of initial rates of Mg^{2+} efflux against increasing isotonic Na^+_o was rather biphasic with saturating effect at around 15 mM Na^+_o (figure 1). The biphasic curve was more clearly shown in the inset, when the data was plotted in the double reciprocal (Lineweaver-Burk) form. Two linear components of Na^+_o -induced Mg^{2+} efflux with different slopes ($p>0.01$) and intercepts ($p>0.01$) appeared. These results suggested that thymocytes were endowed with two Na^+_o/Mg^{2+}_i exchangers with different affinities for external sodium.

Loading the cells with Mg^{2+} markedly increased the rate of Na^+_o –dependent Mg^{2+} efflux at both high and low Na^+_o. As shown in figure 2, the efflux of Mg^{2+} stimulated by Na^+_o in Mg^{2+}-loaded thymocytes apparently fitted a saturable function of $[Na^+]_o$, according to the equation:

$$V_{Mg}(Na)=V_{Mg}(Na)_{max}[1+(K_{Na}/[Na^+]_o)] \quad (1)$$

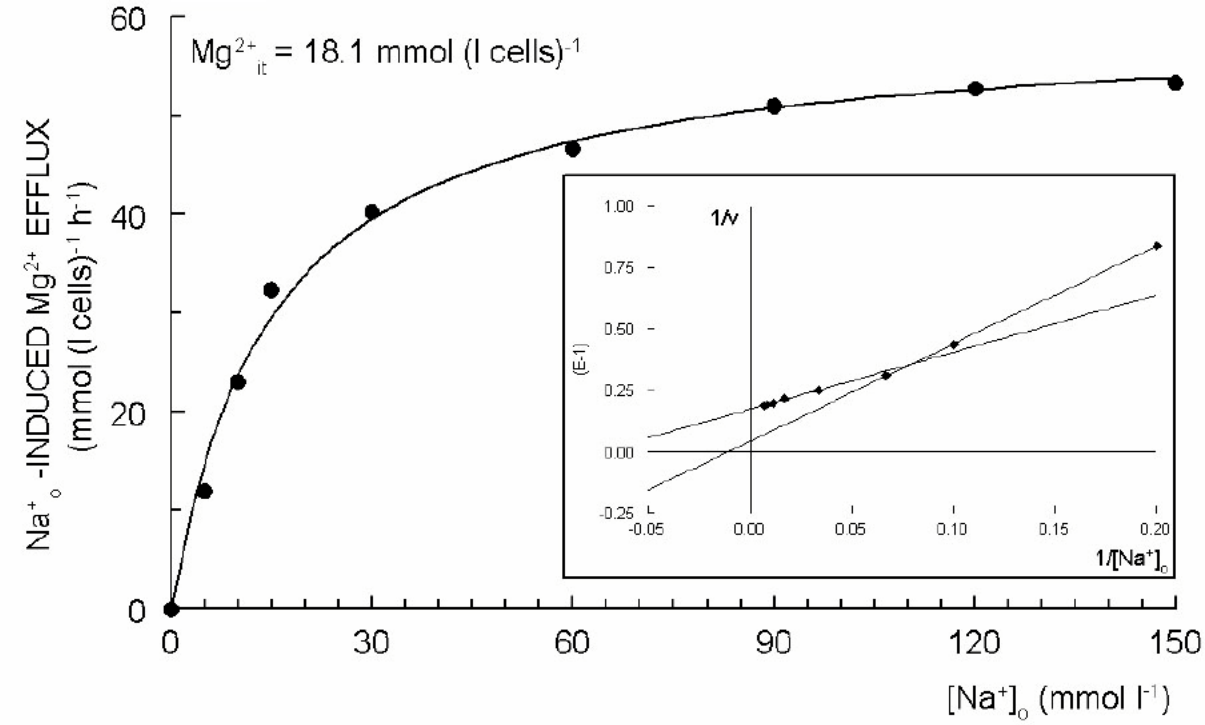

Figure 2. Effect of Na^+_o on Na^+_o–induced Mg^{2+} efflux in Mg^{2+}-loaded thymocytes. The Mg^{2+}_{it} of thymocytes was raised as described in Methods. In this representative trace Mg^{2+}_{it} was 18.1 mM. The activity was initiated incubating the cells in Na^+/choline mixtures and after 5 minutes at 37°C, the sample was centrifuged and the Mg^{2+} present in the supernatants determined. In time-course experiments, the activity was linear for 5 minutes (not shown). Each point is the mean of two single cell tubes. The curve apparently seems to fit the Michaelis-Menten model ($p>0.01$), but linear regression analysis also shows two regression lines with different slopes for high and low $[Na^+]_o$. (inset). At low Na^+_o, the Mg^{2+} efflux fitted the equation $1/V_{Mg}(Na) = 0.004 + 0.40\ 1/[Na^+]_o$ ($r = 0.9999$, $p<0.01$) while at high Na^+_o, the Mg^{2+} efflux fitted $1/V_{Mg}(Na) = 0.02 + 0.20\ 1/[Na^+]_o$ ($r = 0.9958$, $p<0.01$) This graph is representative of 16 experiments.

where $V_{Mg}(Na)$ is the initial rate of Na^+_o-induced Mg^{2+} efflux (in mmol Mg^{2+} (l cells)$^{-1}$ h^{-1}) for each external Na^+ concentration; $V_{Mg}(Na)_{max}$ is the apparent maximal rate at saturating $[Na^+]_o$ and K_{Na} is the apparent dissociation constant for external sodium (in mmol l^{-1} Na^+_o). $V_{Mg}(Na)_{max}$ and K_{Na} were 59.2 mmol Mg^{2+} (l cells)$^{-1}$ h^{-1}and 15.0 mmol Na^+_o l^{-1}, respectively (experiment of figure 2). Even though this result suggested the prevalence of a single Na^+/Mg^{2+} exchanger, the double reciprocal plot revealed again two linear components of Na^+_o-induced Mg^{2+} efflux with different slopes ($p>0.01$) and intercepts ($p<0.01$). These evidence supported the hypothesis that thymocytes have two Na^+_o/Mg^{2+}_i exchangers with different affinities for external sodium, and that they were active both at physiological Mg^{2+}_{it} and when the cells had an enhanced Mg^{2+}_{it} content.

4.4. Dependence of Na^+_o-induced Mg^{2+} efflux on internal Mg^{2+}_{it}

Figure 3 shows the effect of Mg^{2+}_{it} on the Na^+_o-induced Mg^{2+} efflux. In this series of experiments, the Na^+_o-induced Mg^{2+} efflux curves were performed with cells obtained from 7 different pools of thymus glands with different Mg^{2+}_{it}. All curves fitted equation 1 and, strikingly, the enhancement of Mg^{2+}_{it} produced an increase in both K_{Na} and $V_{Mg}(Na)_{max.}$ In the later case, $V_{Mg}(Na)_{max}$ increased exponentially as a function of Mg^{2+}_{it} (inset, figure 3). The remarkable stimulation (trans-stimulation) by Mg^{2+}_{it} was consistent with the fact that the Na^+-induced Mg^{2+} efflux was stimulated by free-magnesium in Mg^{2+}-loaded thymocytes (18). Thus, it was reasonable to assume that, if internal buffers are saturated, further increases in total Mg^{2+} content would be related to corresponding increases in free cytosolic Mg^{2+} (see figures 4C and 4D).

To further study the *trans*- stimulatory effect of Mg^{2+}_{it} and their effects on the putative high and low affinity exchangers, we made experiments with the same pool of cells with high and low Mg^{2+}_{it} (figure. 4A) and analyzed their kinetic properties. Expectedly, the double reciprocal plot of $1/V_{Mg}(Na)$ against $1/[Na^+]_o$ revealed the two linear apparent components of the Na^+_o-induced Mg^{2+} efflux with different slopes and intercepts for high and low Na^+_o (figure. 4B). Comparison of regression lines revealed that the slopes of the reciprocal of the Mg^{2+} efflux induced by sodium in a high range of Na^+_o (30, 60, 90 and 150 mmol l^{-1}) were parallel, that is, there were not significant differences between slopes values (table 1). It implied that the slopes, which in a Linaweawer-Burk plot represent the $K_{Na}/V_{Mg}(Na)_{max}$ ratio (see below), were independent from Mg^{2+}_{it}. This is a property of ping-pong antiporters and enzymes (see Discussion). In contrast, the slopes of the reciprocal of the Mg^{2+} efflux induced by low a range of Na^+_o (5, 10, 15 and 30 mmol l^{-1}) converged ($p<0.01$ between

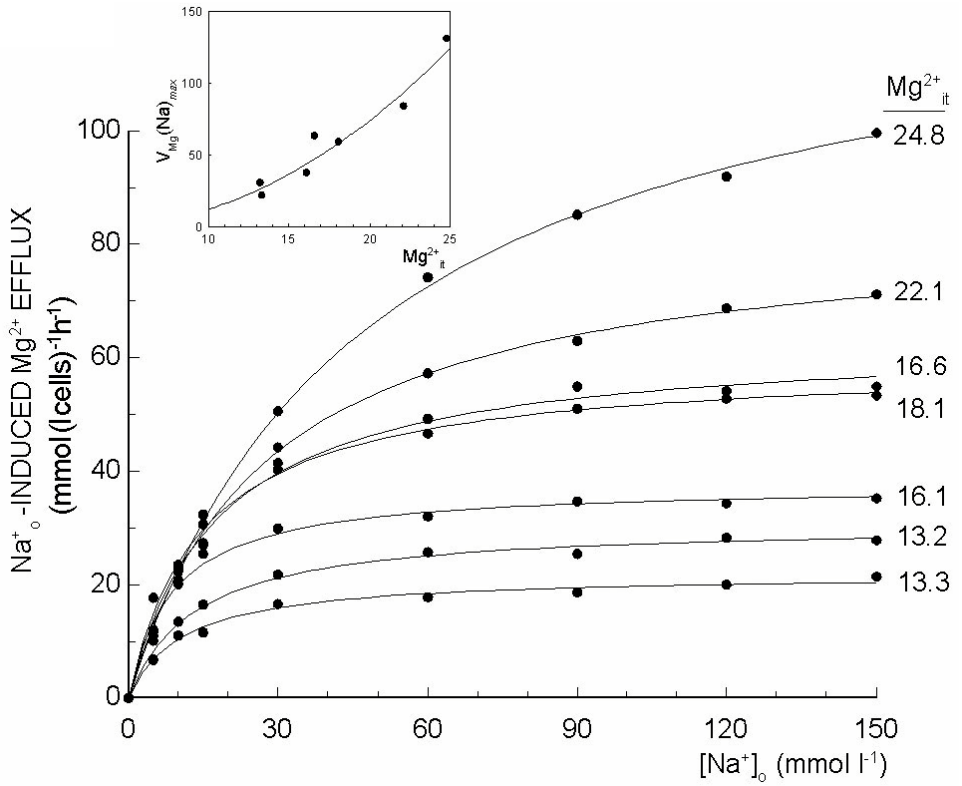

Figure 3. Effect of Mg^{2+}_{it} on Na^+_o–induced Mg^{2+} efflux. Mg^{2+}_{it} (indicated at the right of each curve) was modified in 7 experiments that were performed on different days and different pool of cells. Each point is the mean of two single cell tubes. The curve in figure 2 is included here. All the curves seem to fit the Michaelis-Menten model ($p<0.01$). Inset: $V_{Mg}(Na)_{max}$ was a function of Mg^{2+}_{it} according with the equation $V_{Mg}(Na)_{max} = (-1.62 + 0.51\ Mg^{2+}_{it})^2$, $r = 0.9714$, $p<0.01$).

Table 1. Linear Regression Coefficients for High and Low range external Na^+ obtained from traces described in figure 4

	High Na_0 (1/30 to 1/150 mmol l^{-1})		**Low Na_0 (1/5 to 1/30 mmol l^{-1})**	
[a]Mg^{2+}_{it}	**Slope**	**Intercept**	**Slope**	**Intercept**
1 High 24.0	0.3430	0.0091	0.2921	0.0106
1 Low 14.9	0.3526 (ns)	0.0454 [c]	0.5651 [c]	0.0391 [c]
2 High 24.2	0.3683	0.0175	0.2999	0.0179
2 Low 16.0	0.4586 (ns)	0.0318 [c]	0.4095 [b]	0.0285 [c]
3 High 30.5	0.3307	0.0295	0.4603	0.0249
3 Low 15.0	0.3841 (ns)	0.0431 [c]	0.5411 [b]	0.0395 [c]
4 High 25.6	0.1537	0.0286	0.2438	0.0260
4 Low 20.0	0.2345 (ns)	0.0324 [c]	0.3013 [b]	0.0328 [c]
5 High 28.6	0.2381	0.0280	0.3238	0.0268
5 Low 18.9	0.2759 (ns)	0.0341 [c]	0.6778 [c]	0.0167 [c]
Mean ± SE	0.3139 ± 0.028	0.0299 ± 0.004	0.4115 ± 0.046	0.0263 ± 0.003

Linear Regression Coefficients for High and Low $[Na^+]_o$ values in 5 pairs of subsets of the same pool of cells with different Mg^{2+}_{it} similar to those described in figure. 4B. The slopes in the second column (High Na^+_o) did not correlate with Mg^{2+}_{it} (first column). The slopes in the third column (High Na^+_o), excepted the highest value, correlated with Mg^{2+}_{it} (first column, $p<0.01$). [a] (mmol (l cells)$^{-1}$); [b] $p<0.05$ and [c] ($p<0.01$) vs. High Mg^{2+}_{it} . $p<0.01$ for all linear regressions, ns not significant

slopes, table 1). It implied that the $K_{Na}/V_{Mg}(Na)_{max}$ ratio was highly dependent from Mg^{2+}_{it}. This is a property of simultaneous antiporters and enzymes. Additionally, the double reciprocal plot of $1/V_{Mg}(Na)$ against $1/Mg^{2+}_{it}$ (at low and high Mg^{2+}_{it}) showed parallel lines at high Na^+_o (figure 4C) while clearly convergent lines appeared at low Na^+_o (figure 4D). It is important to mention that, even when Mg^{2+}_{it} might not represent the actual free Mg^{2+} concentration in the cytoplasm, the results depicted in figures 4C and 4D showed that the kinetic properties that define ping pong or simultaneous exchangers (parallelism or convergence) are similar when $1/V_{Mg}(Na)$ is plotted either against $1/Na^+$ or against $1/Mg^{2+}_{it}$. This strongly supported the hypothesis that thymocytes have two Na^+_o/Mg^{2+}_i exchangers which differ in their mechanistic (ping-pong and simultaneous models).

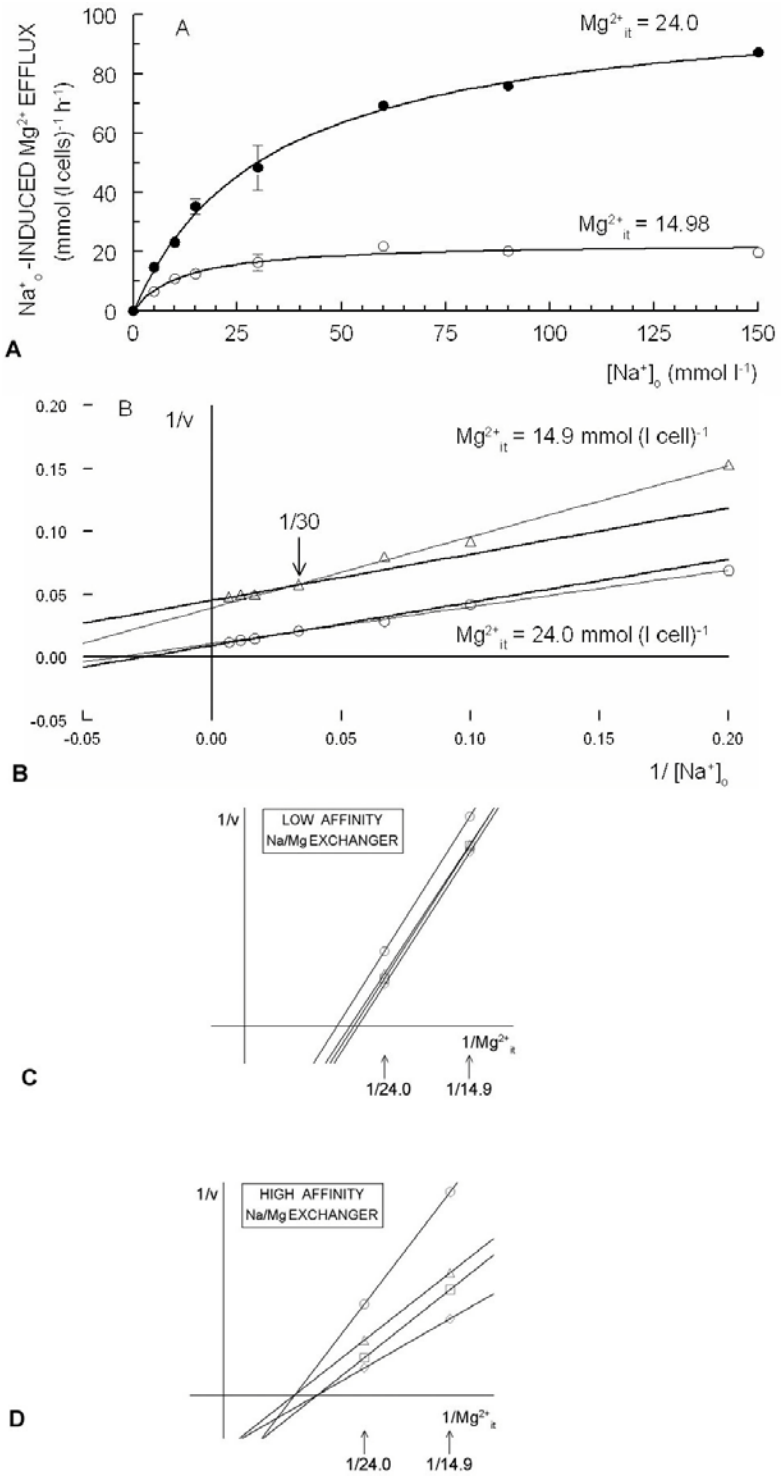

Figure 4. A) Effect of Mg^{2+}_{it} on Na^+_o–induced Mg^{2+} efflux in a pair of subsets of the same pool of cells modified to obtain different Mg^{2+}_{it} (14.9 and 24 mmol l^{-1}). Both curves, for high and low Mg^{2+}_{it} seem to fit the Michaelis-Menten model ($p<0.01$). Each point is the mean ± S.E. of two measurements. B) The double reciprocal plot (the inverse of the Mg^{2+} flux against the inverse of $[Na^+]_o$) at high and at low Mg^{2+}_{it} shows four regression lines with different slopes ($p<0.01$) for high $[Na^+]_o$ values (30 to 150 mmol l^{-1}) and low values (5 to 30 mmol l^{-1}). Notice that lines for high $[Na^+]_o$ were parallel (not different slopes, $p<0.01$) regardless of Mg^{2+}_{it}, whereas that in the low range of $[Na^+]_o$ lines at high and low Mg^{2+}_{it} tend to converge (different slopes, $p<0.01$). C) The double reciprocal plot of the inverse of the Na^+_o-induced Mg^{2+} efflux against the inverse of Mg^{2+}_{it} shows parallel lines for high $[Na^+]_o$ values (30 to 150 mmol l^{-1}). D) The same plot as in C, obtained with low $[Na^+]_o$ values (5-30 mmol l^{-1}) shows convergent lines. This set of graphs is representative of 5 experiments (see table 1).

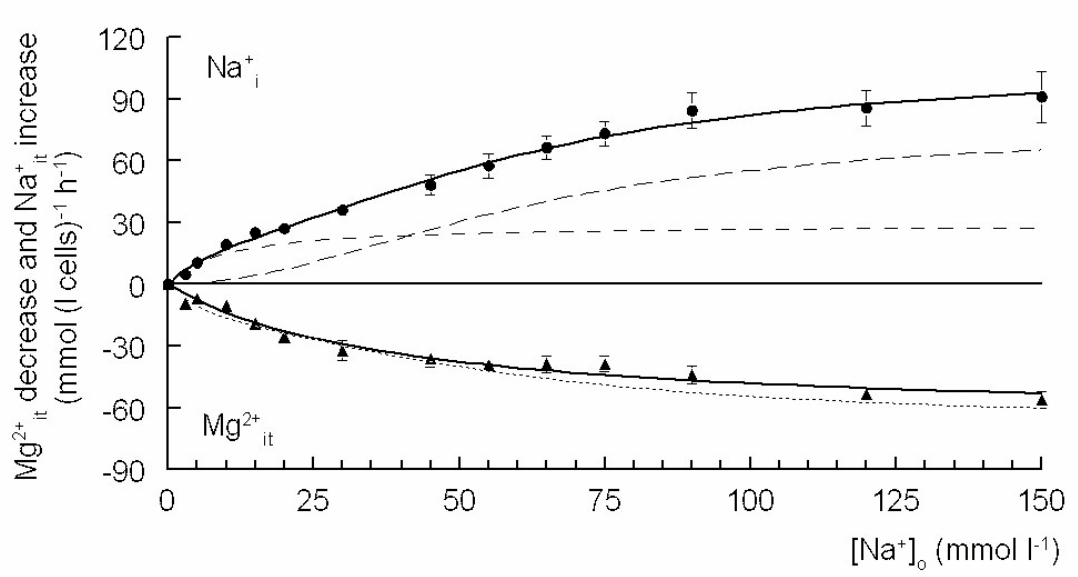

Figure 5. Effect of external sodium (Na^+_o) on Na^+_{it} increase (filled circles) and Mg^{2+}_{it} decrease (filled triangles) in Mg^{2+}-loaded thymocytes. Mg^{2+}-loaded thymocytes were incubated in isotonic mixtures of choline-NaCl supplemented with $2•10^{-3}$ M ouabain + 10^{-4} M bumetanide, at 37 °C. After 5 minutes incubation the cells were centrifuged, the resultant pellet was lysed, and the Na^+ and Mg^{2+} content quantified as described in Methods. Each point is the mean ± S.E. of three single cell tubes. Curves were fitted by using the Levemberg-Marquardt algorhythm. The continuous line in the curve of Na^+ represents the computed equation 3 for two transporters, which are individually described by the dashed lines. The hyperbolic line fits a $1Na^+/1Mg^{2+}$ exchanger, whereas the sigmoid line fits a $2Na^+/1Mg^{2+}$ exchanger. The continuous line in the Mg^{2+}_{it} curve on the bottom seems to fit the measured Mg^{2+}_{it} decrease to a single michaelian component. The dotted point that overlaps this curve represents the theoretical Mg^{2+}_{it} decrease corresponding to the sum of the Mg^{2+} exchanged for Na^+ through the $1Na^+/1Mg^{2+}$ exchanger and the Mg^{2+} exchanged for half the Na^+ transported through the $2Na^+/1Mg^{2+}$ exchanger. The goodness of the fitting was tested by comparing the R-Squared and the Mean Square Error of the regression for the two transporters model (equation 3) adjusted for (n-4) degrees of freedom and those which were obtained from a single transporter model fitting to the Michaelis-Menten equation adjusted for (n-2) degrees of freedom. The adjusted R-Squared were 98.03 ± 0.46% and 97.34 ± 0.66% for the two exchangers model and for a single exchanger model, respectively ($p>0.05$, paired signed rank test, n = 8). The Mean Square Error were 17.73 ± 3.86 and 24.13 ± 5.62 for the two exchangers and a single exchanger models, respectively ($p>0.05$, paired signed rank test, n = 8). Mean ± S.E. of 8 experiments.

4.5. Induction of Mg^{2+}_{it} decrease and Na^{2+}_{it} increase by Na^+_o in Mg^{2+}-loaded thymocytes

Fresh (with normal Mg^{2+}_{it}) thymocytes showed small Na^+_o-induced outward Mg^{2+} fluxes (figure 1) and did not present significant increases in Na^+_{it} in the presence of ouabain (2×10^{-3} M) and bumetanide (10^{-4} M) (not shown), which inhibit the Na^+/K^+ATPase and the $Na^+,K^+,2Cl^-$ cotransport, respectively. Likewise, in Mg^{2+}-loaded thymocytes, the Na^+_o-dependent Mg^{2+}_{it} decrease occurred without significant Na^+_{it} increase indicating the Na^+/K^+ATPase was active (not shown). However, in the presence of 2×10^{-3} M ouabain and 10^{-4} M bumetanide, a significant Na^+_{it} increase occurred, concomitantly with the Na^+_o-induced Mg^{2+}_{it} decrease (figure 5). This evidence indicated that, as expected, the Mg^{2+} efflux detected in Mg^{2+}-loaded thymocytes was coupled to Na^+ influx.

Strikingly, the Na^+_o-induced Na^+_{it} increase showed a biphasic curve with an inflexion close to 30 mM Na^+_o. This suggested that Na^+ was transported into the cell by the two distinct Na^+/Mg^{2+} exchangers with different affinities for Na^+_o, which became evident from experiments made in fresh and Mg^{2+}-loaded cells (figures 1, 2 and 4). We named them HANao and LANao, (acronyms of High- or Low- Affinity for Na^+_o, respectively). To obtain approximate values for the respective maximal rates and dissociation constants, the curves of Na^+_{it} increase in 8 experiments were tested to fit the following equation, which has two terms that define two different saturable transport systems:

$$V_{Na}(Na_T) = V_{Na}(Na_H)_{max} / [1 + (K_{Na\,H}/[Na^+]_o)^a] + V_{Na}(Na_L)_{max} / [1 + (K_{Na\,L}/[Na^+]_o)^b] \quad (3)$$

Where $V_{Na}(Na_T)$ is the measured Na^+_o-induced Na^+_{it} increase rate (in mmol Na^+ (l cells)$^{-1}$ h^{-1}) for each $[Na^+]_o$; $V_{Na}(Na_H)_{max}$ and $V_{Na}(Na_L)_{max}$ are the maximal rates (in mmol Na^+ (l cells)$^{-1}$ h^{-1}) carried out independently through the high- and the low- affinity for Na^+_o exchangers, respectively; $K_{Na\,H}$ and $K_{Na\,L}$ are the apparent dissociation constants for Na^+_o (in mmol Na^+ l^{-1}) for Na^+_o of high- and low- exchangers, respectively; and a and b are coefficients (with arbitrary values of 1, 2 or 3) representing the fraction of Na^+ ions transported for each exchanger. The best fit using the Levemberg-Marquardt algorithm (continuous line, figure 5) was found for $a = 1$ and $b = 2$; where $V_{Na}(Na_H)_{max}$ and $V_{Na}(Na_L)_{max}$ were 30.5 ± 6.1 and 79.5 ± 14.3 mmol Na^+ (l cells)$^{-1}$ h^{-1}, respectively; and $K_{Na\,H}$ and $K_{Na\,L}$

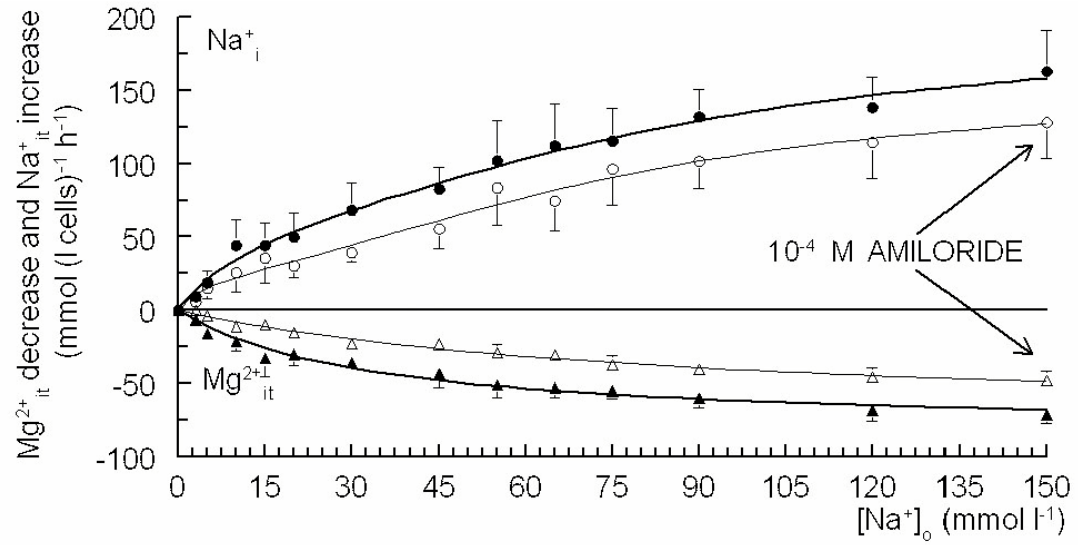

Figure 6. Amiloride (10^{-4} M, open symbols) inhibited at similar extent Na^+_o–induced Na^+ content increase and Na^+_o–induced total Mg^{2+} content decrease at both high and low $[Na^+]_o$ values. The 4 curves had the same amount of DMSO (< 0.01%). The rest of the experimental conditions are described in figure 5. Mean ± S.E. of three experiments.

Table 2. Dependence on $[Na^+]_o$ of the stoichiometry of the Na_o/Mg_i exchange

$[Na^+]_o$(mM)	0	3	5	10	15	20	30	45	55	65	75	90	120	150
$[Na]_{it}/[Mg]_{it}$	0	0.68	1.21*	1.26*	1.23*	1.08	1.04	1.50#	1.40	1.62#	1.78#	1.81#	1.69#	1.82#
± S.E.	0	0.07	0.03	0.08	0.06	0.05	0.05	0.1	0.1	0.05	0.05	0.05	0.05	0.06

The Na^+_{it}/ Mg^{2+}_{it} ratios were calculated from the Na^+_{it} increase and the Mg^{2+}_{it} decrease induced by the indicated external sodium concentration ($[Na^+]_o$) under initial rate conditions, in Mg^{2+}-loaded thymocytes. The initial Na^+_{it} and Mg^{2+}_{it} were 8.61 ± 0.76 and 20.76 ± 1.03 mmol (l cells)$^{-1}$, respectively. The ratios are means ± SE (n=10)

were 9.2 ± 1.6 and 65.1 ± 8.7 mmol Na^+ l^{-1}, respectively (n=8). The hyperbolic dashed line represents the computed equation (3) for the $HANa_o$ with $a = 1$:

$$V_{Na}(Na_H) = V_{Na}(Na_H)_{max}/[1+ (K_{Na\,H}/[Na^+]_o)^1] \quad (4).$$

and the sigmoid dashed line represents the computed equation (4) for the $LANa_o$, with $b = 2$.

$$V_{Na}(Na_L) = V_{Na}(Na_L)_{max}/[1+ (K_{Na\,L}/[Na^+]_o)^2] \quad (5).$$

Consistently, the Na^+_o-induced Mg^{2+}_{it} decrease (in the presence of bumetanide and ouabain) was quantitatively similar to the Na^+_o-induced Mg^{2+} efflux, when detected in the medium (figure 2). However, unlike the Na^+_o-induced Mg^{2+} increase detected in the medium (figure 2, inset), the biphasic curve could not be resolved for Na^+_o-induced Mg^{2+}_{it} decrease, not even in double reciprocal plots (not shown), instead, the non –linear regression analysis showed that the Na^+_o-induced Mg^{2+}_{it} decrease fitted the Michaelis-Menten model (see Discussion).

The model of two antiporters with coupled $1Na^+/1Mg^{2+}$ and $2Na^+/1Mg^{2+}$ stoichiometries requires, as a necessary condition, that the amount of Mg^{2+} coupled with Na^+_o influx equals the measured Mg^{2+}_{it} decrease. The dotted line on the lower part of figure 5 reflects the sum of the amount of Mg^{2+} exchanged by Na^+ through the $1Na^+/1Mg^{2+}$ plus a half of the amount of Mg^{2+} exchanged by Na^+ through the $2Na^+/1Mg^{2+}$, according with the equation 6:

$$V_{Na}(Na_T) = [-V_{Na}(Na_H)_{max}/(1+ (K_{Na\,H}/[Na^+]_o)] + ½[-V_{Na}(Na_L)_{max}/(1+ (K_{Na\,L}/[Na^+]_o)^2)] \quad (6)$$

Consistently, figure 5 shows that the dotted line clearly overlapped the measured decrease in Mg^{2+}_{it}. Furthermore, the quantification of Na^+_{it} and Mg^{2+}_{it} permitted to establish the stoichiometry of the Na^+/Mg^{2+} exchange under initial rate conditions. The Na^+_{it}/Mg^{2+}_{it} relationship was near 1 at low Na^+_o and increased steeply toward 2 as the Na^+_o was raised (table 2). These values coincided with the constants *a* and *b* obtained by iteration of equation 3.

4.6. Inhibition by amiloride of either Na^+_o-induced Mg^{2+} efflux and Na^+_o-induced Na^+ influx in Mg^{2+}-loaded thymocytes

We used the Na^+/Mg^{2+} exchange inhibitor amiloride (12, 16, 17, 22) to further test whether the Na^+_o-induced Mg^{2+} efflux and the Na^+_o-induced Na^+ influx were indeed coupled. The IC_{50} of amiloride on the Na^+_o–induced Mg^{2+} efflux was 2.60 ± 0.60 × 10^{-4} M and 10^{-3} M completely inhibited Mg^{2+} outward fluxes induced either by low (30 mmol l^{-1}) and high (150 mmol l^{-1}) Na^+_o (not shown). As expected for a Na^+/Mg^{2+} exchange inhibition, a submaximal (10^{-4} M) amiloride concentration produced a comparable inhibition of Na^+_o–induced Mg^{2+} efflux and Na^+_o–induced Na^+ influx (figure 6). Furthermore, this inhibition was similar at both high and low Na^+_o, suggesting that HANao and LANao were similarly sensitive to this inhibitor.

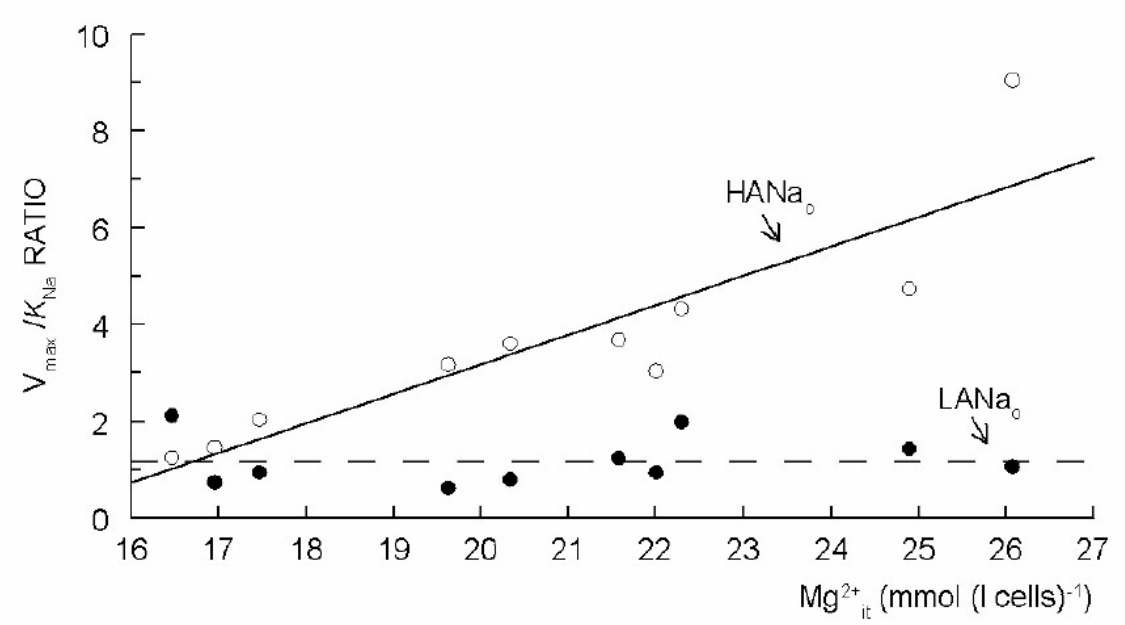

Figure 7. Plot of $V_{Na}(Na)_{max}/K_{Na}$ ratio vs. Mg^{2+}_{it} for the Na^+/Mg^{2+} exchanger with high affinity for external Na^+ (HANao) and for the Na^+/Mg^{2+} exchanger with low affinity for Na^+_o (LANao). $V_{Na}(Na)_{max}$ and K_{Na} at each Mg^{2+}_{it} were computed from experiments shown in table 2.

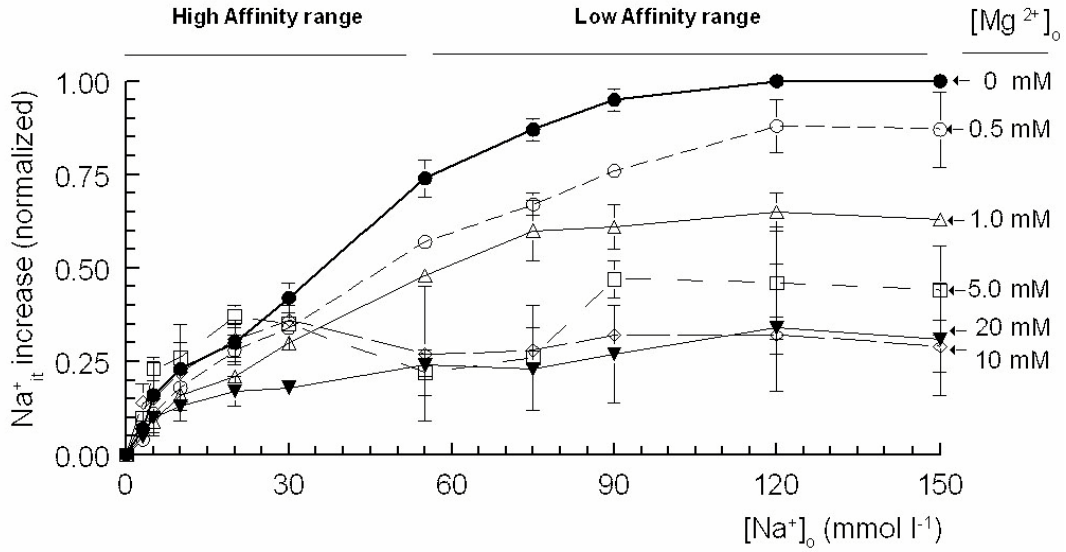

Figure 8. Inhibitory effect of external magnesium on the Na^+_o-induced Na^+_{it} increase. Measurements of Na^+_{it} induced by external sodium in Mg^{2+}-loaded cells were performed in the presence of different amounts of external magnesium (indicated at the right of each curve). The rest of the experimental conditions are described in figure 5.

4.7. Dependence of the $V_{Mg}(Na)_{max}/K_{Na}$ ratio to the internal Mg^{2+} content

The lack of dependence of the ratio between the maximal rate and the dissociation constant for any substrate (K_m) on the concentration of the other substrate has been proposed as a condition for ping-pong models (26-29) (see Discussion). Figure 7 shows that the $V_{Na}(Na_H)_{max}/K_{Na\,H}$ (high affinity) ratio (obtained from experiments of table 2) was a linear function of the Mg^{2+}_{it} ($y = -9.02 + 0.61\ Mg^{2+}_{it}$, $p<0.01$). In a marked contrast, the $V_{Na}(Na_L)_{max}/K_{Na\,L}$ nor its 2nd power (in accordance with the $2Na^+/1Mg^{2+}$ stoichiometry) was constant for each Mg^{2+}_{it} . These evidence indicated that $LANa_o$ behaved like a ping-pong system whereas the $HANa_o$ behaved as a simultaneous exchanger (see Discussion).

Furthermore, the Na^+ influx was clearly inhibited by Mg^{2+}_o in a concentration–dependent way only when Na^+_o was higher than 30 mmol l^{-1}, suggesting a *cis* - competitive behavior between Mg^{2+}_o and Na^+_o for the external binding site of LANao (figure 8). Interestingly, 1

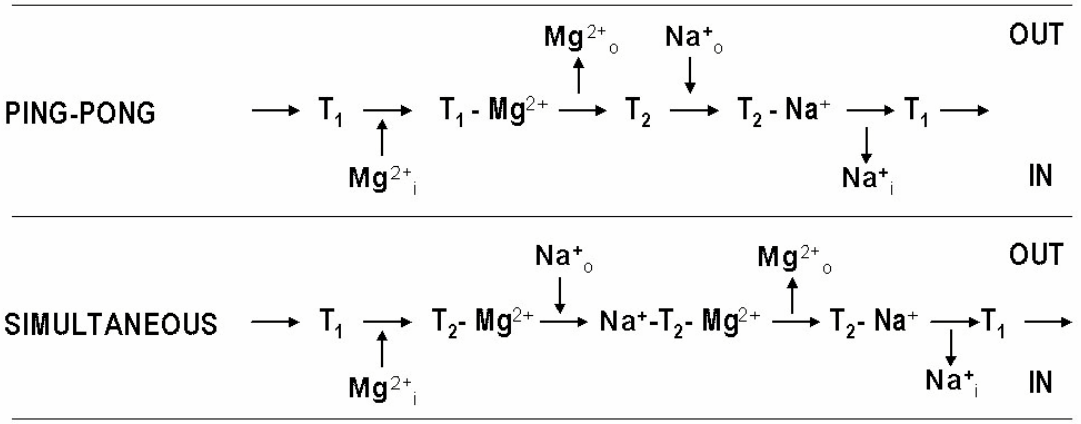

Figure 9. Schematic representation of simultaneous and ping pong modes of exchange. In the ping-pong system one ion is bound at a time, because it has only a binding site for both ions. Consequently, binding of Mg^{2+} does not modify the affinity for Na^+. For this reason, the $V_{Na}(Na)_{max}/K_{Na}$ ratio is constant at each Mg^{2+}_{it}. In the simultaneous system, both ions can be simultaneously bound to the exchanger, forming a ternary complex. Thus, binding of Mg^{2+} modifies the affinity of the exchanger for Na^+. For this reason, the $V_{Na}(Na)_{max}/K_{Na}$ ratio depends on Mg^{2+}_{it}.

mmol l^{-1} Mg^{2+}_o, (similar to the plasma Mg^{2+}-free concentration) induced ~50% of inhibition on the Na^+ influx through this exchanger. In contrast, Mg^{2+}_o did not affect the Na^+_o-induced Na^+ influx through HANao, except at 20 (figure 7) and 40 mmol l^{-1} (not shown). These later effects could be related to a reduction of the Mg^{2+} gradient.

4.8. Thermodynamics of the Na^+/Mg^{2+} exchange

In this work, the Mg^{2+} efflux experiments were performed under zero-trans conditions, in a similar way than previous kinetic studies (10-12). However, we calculated the reversal potential for Na^+/Mg^{2+} exchangers in thymocytes under physiological conditions in equilibrium according with Nernst's Equation:

$$(E_{ion}) = 61.4/z \text{ mV } \log([ion]_o/([ion]_i)$$

Since $[Na^+]_o$ and Na^+_{it} are 145 and 9.87 mM, respectively and $[Mg^{2+}]_o$ and free $[Mg^{2+}]_i$ are ~1 and 0.38 mM (18), respectively, the reversal potentials for $1Na^+/1Mg^{2+}$, $2Na^+/1Mg^{2+}$ and $3Na^+/1Mg^{2+}$ exchangers are 46.9, 119.9 and 192.7 mV, respectively. Since membrane potential in rat thymocytes is E_m = -45.4 ± 3.8 mV (19), the driving force ($\Delta\mu = E_m - E_{Na/1Mg}$) is higher than 0 and, consequently Mg^{2+} should be extruded out of the thymocyte at physiological conditions in all the three possible stoichiometries.

5. DISCUSSION

Atomic Absorption techniques, along with the modification of the intracellular magnesium content, have been used to study the kinetics and the properties of the Na^+/Mg^{2+} exchange by several authors (10-13). However, this method presents the considerable disadvantage that total internal concentration, and not only the ionized fraction, is measured. In the present work we have attempted to overcome this disadvantage by studying the Na^+/Mg^{2+} exchange through the analysis of $[Mg^{2+}]$ on the external medium, so that actual values of Mg^{2+} exchanged by Na^+ were detected, and also through the analysis of the increase on the Na^+ content, which is present as a free cation (not compartmented) in the cell. This approach, along with the determination of Na^+_o-induced Mg^{2+}_{it} decrease; have unveiled the presence of two exchangers in thymocytes that have different affinities for Na^+ (HANao and LANao) and different mode of action.

The biphasic curve of Na^+_o-induced Na^+_{it} increase in Mg^{2+}-loaded thymocytes, and quantitative data shown in table 2, strongly indicate that HANao follows a Michaelian model with a $1Na^+/1Mg^{2+}$ stoichiometry and that LANao fits a sigmoidal behavior with a $2Na^+/1Mg^{2+}$ stoichiometry. However, the Na^+_o-induced biphasic Na^+_{it} increase was not accompanied by a clear biphasic Mg^{2+}_{it} decrease. It should be noted that, unlike Na^+, both exchangers extrude only $1Mg^{2+}$ at any Na^+_o for each exchange cycle. Consequently, whereas the Na^+ influx as a function of Na^+_o may be expected to be biphasic, the Na^+_o-induced curves of Mg^{2+}_{it} decrease and Mg^{2+} efflux should not necessarily display a biphasic curve.

5.1. Simultaneous versus ping-pong exchange

Although it has been often difficult to distinguish between ping-pong and simultaneous enzymes or exchangers, it is generally accepted that ping-pong systems must fulfil two requirements:

1) For a ping-pong antiporters, the $V_{Na}(Na_L)_{max}/K_{Na\ L}$ ratio must be independent on the *trans* ion concentration (Mg^{2+}_{it}). It implies that only one substrate is bound to the exchanger at a time on the binding site, which is alternately exposed facing in or facing out of the cell (figure 9). Consequently, the binding to the first substrate (Mg^{2+}_i) does not modify the affinity for the second one (Na^+_o). In contrast, a simultaneous system binds both substrates sequentially forming a ternary complex, so that binding of the 1st (Mg^{2+}_i) affects the affinity of the complex for the 2nd one (Na^+_o).

We show here that LANao behaves like a

ping-pong by two different ways:

1) The lack of dependence from Mg^{2+}_{it} of the Na^+/Mg^{2+} exchange on the basis of the kinetic analysis of the double reciprocal plots of Na^+_o-induced Mg^{2+} efflux curves (figures 4A, 4B and 4C, notice that the slopes of the parallel lines are $K_{Na}/V_{Na}(Mg)_{max}$), and the lack of dependence from Mg^{2+}_{it} of the $V_{Na}(Na)_{max}/K_{Na}$ ratio obtained by iteration of equation 3 of the biphasic curves of Na^+_o-induced Na^+ influx curves (figure 7). In contrast, HANao behaves like a simultaneous antiporter according to the following evidence: a) The lines on the double reciprocal plots of Na^+_o-induced Mg^{2+} efflux curves (figures 4B and 4C) are convergent implying that the slopes are modified by Mg^{2+}_{it} and b) the dependence from Mg^{2+}_{it} of the $V_{Na}(Na)_{max}/K_{Na}$ ratio obtained by iteration of equation 3 of the biphasic curves of Na^+_o-induced Na^+ influx curves (figure 7).

2) The *trans* ion (Mg^{2+}_i) on the *cis* side inhibits the exchange. In a ping pong system, the external site for Na^+ should be exposed once the internal Mg^{2+} is translocated out of the cell. If Mg^{2+} is present in the external side, binding of Na^+ is blocked by Mg^{2+}, resulting in Na^+/Mg^{2+} exchange inhibition. It happens with LANao but not with HANao (figure 8). Furthermore, the strong inhibition induced by very low Mg^{2+}_o at maximal Na^+_o clearly rules out that the Na^+ influx might be the result of some uncoupled uptake in Mg^{2+}-loaded cells.

These characteristics strongly suggest that LANao and HANao have ping pong and simultaneous mechanism of Na^+/Mg^{2+} exchange, respectively. An interesting question derived from these findings is whether LANao and HANao are different structural entities or, by contrast, the Na^+/Mg^{2+} exchange is performed by an unique antiporter working with two stoichiometries in response to high or low Na^+_o. We consider that it is highly improbable that a protein exchanger switch the number of binding sites in order to form binary or ternary compounds with the substrates. The most plausible hypothesis is that HANao and LANao are two different transporters.

5.2. Physiological roles of ping pong and simultaneous Na^+/Mg^{2+} exchangers coexisting in the same cell

There is a number of ion exchangers that follow the sequential or ping-pong translocation mechanism. That is the case for the AE-1 anion carrier (26, 28, 29), the Na^+/Li^+ countertransport found in human red blood cells (27) or the Na^+/Ca^{2+} exchanger (30). In this paper we show for the first time a ping-pong mechanism in a Na^+/Mg^{2+} exchanger and that it coexist with a simultaneous transporter in the same cell. The properties of the high-$1Na^+/1Mg^{2+}$ and the low-affinity $2Na^+/1Mg^{2+}$ suggest interesting functional implications for a cell possessing both transporters. The high affinity simultaneous transporter (HANao) would serve to maintain the relatively low, steady -state intracellular Mg^{2+} found in resting levels. In normal conditions, the low-affinity ping-pong transporter (LANao) must be considerably inhibited, ~ 50 %, at normal external free Mg^{2+} (0.5-1 mM). This exchanger (LANao), which seems to be the main contributor of the exchange in Mg^{2+}-loaded cells, would be activated only when the Mg^{2+} content reaches abnormally high values.

Our present results further confirm previous findings which suggest that Mg^{2+}-loaded, Ca^{2+}-depleted thymocytes display Na^+/Mg^{2+} exchangers with different stoichiometries (18). In these studies the Na^+/Mg^{2+} exchange detected by Magfura-2 fluorescence required the use of Ca^{2+} -depleted cells because Ca^{2+}, at nanomolar concentration, masks milimolar changes in Mg^{2+} (31-35). It is possible that cytosolic Ca^{2+} may have a regulatory role on Na^+/Mg^{2+} exchangers, perhaps through phosphorylative processes. However, we have found trans-stimulation and evidence for different Na^+/Mg^{2+} stoichiometries under conditions in which the intracellular Ca^{2+} was under 10^{-7} M (because the presence of EGTA, 18) and when no EGTA was present and contaminating Ca^{2+} was $\sim 10^{-5}$ M (this work). These evidence suggests that intracellular calcium does not play a fundamental role in sustaining the exchange activity of both exchangers. Whether or not the intracellular calcium modulates the Na^+/Mg^{2+} exchangers remains to be established.

In summary, two Na^+_o/Mg^{2+} exchangers, $HANa_o$ and $LANa_o$, were dissected in the rat thymocyte according to their differences in stoichiometry, affinity for Na^+_o and mechanism of exchange. The remarkable stimulation by internal Mg^{2+} on the additive outward Mg^{2+} fluxes endows the thymocyte with a notable ability to maintain the large Mg^{2+} electrochemical gradient across the cell membrane.

5.3. Appendix: The kinetics of a bisubstrate exchanger

Our study raises the question whether it is actually possible to derive kinetic and thermodynamic calculations even if we do not know the cytosolic Mg^{2+} fraction of the Mg^{2+}-loaded rat thymocytes. The argument supporting our study is based in the one used to study the Na^+/Mg^{2+} exchange in human re blood cells (10, 12) and takes into consideration the following. A bisubstrate enzymatic reaction is ruled by the following general equation:

$$v = V_{AB\ max\ max}(1+ (K^A_m/[A])+ (K^B_m/[B])+ (K^A_s\ K^B_m/[A][B])$$

where A and B are the substrates and [A] and [B] are their respective concentrations; $V_{AB\ max\ max}$ is the limiting maximal rate for saturating [A] and [B]; K^A_m and K^B_m are the limiting Michaelis -Menten's constants for A and B, respectively, and K^A_s is the dissociation constant for A. In the case of ping-pong reactions, the protein does not form ternary complexes (that requires binding of both substrates before catalyzing the translocation) and the equation is simplified to:

$$v = V_{AB\ max\ max}(1+ (K^A_m/[A])+ (K^B_m/[B])$$

On the other hand, if only one of the substrates is measured while the concentration of the second remains constant (as in case of an exchanger under initial rate conditions); the kinetics of the measured substrate fits a single Michaelis-Menten's model. Thus, if outward fluxes

of substrate B (Mg^{2+} in our case) are stimulated by increasing $[A_o]$ (Na^+ in our case) and Na^+_o–induced Mg^{2+} efflux (ie.$V_A(B)$) are measured under initial rate conditions, they will fit the equation:

$$v_A(B) = V_A(B)_{max}/(1+K_{A\,0.5}/[A_o])$$

The concentration of [B] being constant during the reaction period measured. The model would be more complex if the stoichiometry is 2A:1B.

$$v_A(B) = V_A(B)_{max}/(1+(K_{A\,0.5}/[A_o])^2)$$

This equation will generate a sigmoid curve, like that proposed for LANao. Finally, if two systems with stoichiometries 1A:1B and 2A:1B are present, the global equation will be

$$v = V_A(B)_{max}/(1+K_{A\,0.5}/[A_o]) + V_A(B)_{max}/(1+(K_{A\,0.5}/[A_o])^2)$$

This equation is similar to the one we used in this work (adapted form Dixon and Web, 36).

Notice that this last equation only allows us to reach approximated values for apparent dissociation constant for external Na^+ because we do not know the value of $(K^A_s\ K^B_m/[A][B])$, which should have been included in the first term for a simultaneous antiporter. We did not obtain it because we did not measure [B] (ie. the initial free cytosolic Mg^{2+} concentration in Mg^{2+}–loaded cells). However, assuming that this value is between 0.6 and 8.0 mM Mg^{2+}_{cyt} in Mg^{2+}-loaded thymocytes (18), the value of $(K^A_s\ K^B_m/[A][B])$ will be reasonably small for high concentrations of Na^+_o

7. ACKNOWLEDGMENTS

This work was supported by DGICYT PB95-1150 and PAI -Andalusian Research Program (Spain). M.T.G-M spent a sabbatical leave at the Universidad de Granada (Spain) which was supported by the Consejo Nacional de Ciencia y Tecnología (CONACYT) (Mexico) and the Dirección General de Asuntos de el Personal Académico (DGAPA) de la Universidad Nacional Autónoma de México (UNAM) (Mexico). We are grateful to Prof. J. D. Luna (Dpto. Bioestadistica, Universidad de Granada, Spain) for statistical advice and Dr. Javier García-Sancho (IBGM, University of Valladolid, Spain) for helpful discussions. C. Contreras-Jurado and N. Sanchez-Morito contributed equally to this paper. C. Contreras-Jurado present address: Max-Planck-Institüt für experimentelle Medizin Hermann-Rein-Str.3.D-37075 Göttingen Germany.

6. REFERENCES

1. Shaul, O, D. W. Hilgemann, J. de-Almeida-Engler, M. Van Montagu, D. Inz and G. Galili: Cloning and characterization of a novel Mg^{2+}/H^+ exchanger. *EMBO J* 18, 3973-3980 (1999)

2. Jung, D.W. and G. Brierley: Cation transport systems in mitochondria: Na^+ and K^+ uniports and exchangers. *J Bioenerg and Biomembr* 26, 527-535 (1994)

3. Eskes, R., B. Antonsson, A. Osen-Sand, S. Montessuit, C. Richter, R. Sadoul, G. Mazzei, A. Nichols, and J. C. Martinou: Bax-induced cytochrome C release from mitochondria is independent of the permeability transition pore but highly dependent on Mg^{2+} ions. *J Cell Biol* 143, 217-224 (1998)

4. Mandel, G., and R. H. Goodman: Cell signaling. DREAM on without calcium. *Nature* 398, 29-30 (1999)

5. Hille, B: Ion channels of excitable membranes. 3rd edition, Sinauer, Sunderland, MA (2002)

6. Laver, D. R., T. M. Baynes and A. T. Dulhunty: Magnesium inhibition of ryanodine-receptor calcium channels: evidence for two independent mechanisms. *J Membr Biol* 156, 213-229 (1997)

7. Murphy, E: Mysteries of magnesium homeostasis. *Circ Res* 86, 245-248 (2000)

8. Flatman, P. W: Mechanisms of magnesium transport. *Annu Rev Physiol* 53, 259-71 (1991)

9. Günzel, D. and W. R. Schlue: Mechanisms of Mg^{2+} influx, efflux and intracellular "muffling" in leech neurons and glial cells. *Magnesium Res* 13, 123-138 (2000)

10. Lüdi, H., and J. Schatzmann: Some properties of a system for sodium-dependent outward movement of magnesium from metabolising human red blood cells. *J Physiol (London)* 390, 367-382 (1987)

11. Féray, J. C. and R. P. Garay: Demonstration of a Na:Mg exchange in human red cells by its sensitivity to tricyclic antidepressant drugs. *Naunyn-Schmiedeberg's Arch Pharmacology* 338, 332-337 (1988)

12. Féray, J. C., and R. P. Garay: A Na^+-stimulated, Mg^{2+} transport system in human red blood cells. *Biochim Biophys Acta* 856, 76-84 (1986)

13. Günther, T. and J. Vormann: Reversibility of Na+/Mg2+ antiport in rat erythrocytes. *Biochim Biophys Acta* 1234, 105-110 (1995)

14. Günther, T. and J. Vormann: Na(+)-dependent Mg2+ efflux from Mg(2+)-loaded rat thymocytes and HL 60 cells. *Magnesium Trace Elements* 9, 279-282 (1990)

15. Rasgado-Flores, H. and H. Gonzalez-Serratos: Plasmalemmal transport of magnesium in excitable cells. *Front Biosci* 5, d866-d879 (2000)

16. Cefaratti, C., A. Romani and A. Scarpa: Characterization of two Mg^{2+} transporters in sealed plasma membrane vesicles from rat liver. *Am J Physiol.* 275, C995-C1008 (1998)

17. Cefaratti, C., A. Romani and A. Scarpa: Differential

localization and operation of distinct two Mg^{2+} transporters in apical and basolateral sides of rat liver plasma membrane. *J Biol Chem* 275, 3772-3780 (2000)

18. Contreras-Jurado, C., M. T. González-Martínez, E. J. Cobos and A. Soler-Díaz: Fluorometric evidence for different stoichiometries for the Na+/Mg^{2+} exchange in Mg-Loaded rat thymocytes. *Front Biosci* 9, 1843-1848 (2004)

19. Soler, A., R. Rota, P. Hannaert, E. J. Cragoe Jr. and R. P. Garay: Volume-dependent K^+ and Cl^- fluxes in rat thymocytes. *J Physiol (London)*, 465, 387-401 (1993)

20. Senn, N. and R. P. Garay: Regulation of Na+ and K+ contents in rat thymocytes. *Am J Physiol* 257, C12-C18 (1989)

21. Arrazola, A., R. Rota, P. Hannaert, A. Soler and R. P. Garay: Cell volume regulation in rat thymocytes *J Physiol (London)* 465, 403-414 (1993)

22. Günther, T. and J. Vormann: Activation of Na+/Mg2+ antiport in thymocytes by cAMP. *FEBS Lett* 297, 132-134 (1992)

23. Pressman, B. C: Biological applications of ionophores. *Annual Rev Biochem* 45, 501-530 (1977)

24. Lew, V. and J. Garcia-Sancho: Measurement and control of intracellular calcium in intact red cells. *Methods Enzymol* 173, 100-112 (1989)

25. Simonsen, L. O: *J Physiol (London)* 313, 34P (Abstr.) (1981)

26. Salhany, J. M. and P. B. Rauenbuehler: Kinetics and mechanism of erythrocyte anion exchange. *J Biol Chem* 258, 245-249 (1983)

27. Hannaert, P. and R. P. Garay: A Kinetic analysis of Na-Li countertransport in human red blood cells. *J Gen Physiol* 87, 353-368 (1986)

28. Knauf, P. A: In: The Red Cell Membrane. Eds. B. U. Raess and G. Tunnicliff, *Kinetics of Anion Transport,* The Humana Press Inc. Clifton NJ (1989)

29. Restrepo, D., B. L. Cronise, R. B. Snyder and P. A. Knauf: A novel method to differentiate between ping-pong and simultaneous exchange kinetics and its application to the anion exchanger of the HL60 Cell. *J Gen Physiol* 100, 825-846 (1992)

30. Hilgemann, D. W., A. Collins, D. P. Cash and G. A. Nagel: Cardiac Na^+-Ca^{2+} exchange system in giant membrane patches. *Ann NY Acad Sci* 639, 126-139 (1991)

31. Alvarez, J., M. Montero and J. García-Sancho: Cytochrome P-450 may link intracellular Ca2+ stores with plasma membrane Ca2+ influx. *Biochem J* 274, 193-197 (1991)

32. Alvarez, J., M. Montero and J. García-Sancho: Cytochrome P450 may regulate plasma membrane Ca2+ permeability according to the filling state of the intracellular Ca2+ stores (1992) *FASEB Journal* 6, 786-792 (1992)

33. Tashiro, M., P. Tursun, T. Miyakazi, M. Watanabe and Konishi M: Effects of membrane potential on Na+ -dependent Mg2+ extrusion from rat ventricular myocytes. *Jpn. J Physiol* 52, 541-551 (2002)

34. Wisdom, D., M. Geada and J. Singh: Characterization of a sodium-dependent magnesium efflux from magnesium-loaded rat pancreatic acinar cells. *Exp Physiol* 81, 367-374 (1996)

35. Zhang, G. H. and J. E. Melvin: Na+-dependent release of Mg2+ from an intracellular pool in rat sublingual mucous acini. *Biol Chem* 271, 29067-29072 (1996)

36. Dixon, M. and E. C. Webb: In: Enzymes. *Enzyme kinetics*, Academic Press, New York, NY, 82-120 (1979)

Key Words: Na/Mg exchange, Ping pong exchanger, Simultaneous exchanger, Amiloride, Thymocytes

Send correspondence to: Dr Agatángelo Soler-Díaz, Departamento de Fisiología, Facultad de Medicina, Avda, Madrid, 13 Granada, E-18012 Spain, Tel: 34-958-243-521, Fax: 34-958-246-179, E-mail: agasoler@ugr.es

http://www.bioscience.org/current/vol10.htm